

1 **Probability distributions of particle hop distance and**
2 **travel time over equilibrium mobile bedforms**

3 **Thomas C. Ashley¹, Robert C. Mahon², Suleyman Naqshband³, Kate C.P.**
4 **Leary⁴, Brandon McElroy¹**

5 ¹Department of Geology and Geophysics, University of Wyoming, Laramie, WY

6 ²Department of Earth and Environmental Sciences, University of New Orleans, New Orleans, LA

7 ³Department of Environmental Sciences, Wageningen University, Wageningen, Netherlands

8 ⁴Department of Geography, UC Santa Barbara, Santa Barbara, CA

9 **Key Points:**

- 10 • Particle travel times over bedforms are exponentially-distributed as proposed for
11 planar beds.
12 • Streamwise and lateral hop distances over bedforms are not Weibull-distributed
13 as proposed for planar beds.
14 • Bedforms increase the variance in streamwise and lateral hop distances and in-
15 crease diffusive-like transport.

Corresponding author: Thomas C. Ashley, tashley22@gmail.com

Abstract

The joint probability distribution of streamwise particle hop distance, lateral particle hop distance, and travel time constrains the relationships between topographic change and sediment transport at the granular scale. Previous studies have investigated the ensemble characteristics of particle motions over plane-bed topography, however it is unclear whether reported distributions remain valid when bedforms are present. Here, we present measurements of particle motion over bedform topography obtained in a laboratory flume and compare these to particle motions over plane-bed topography with otherwise similar conditions. We find substantial differences in particle motion in the presence of bedforms that are relevant to macroscopic models of sediment transport. Most notably, bedforms increase the standard deviation of streamwise and lateral hop distances relative to the mean streamwise hop distance. This implies that bedforms increase the streamwise and lateral diffusion lengths and, equivalently, increase diffusive-like fluxes.

1 Introduction

The joint probability distribution of particle hop distance and travel time encapsulates the relationship between granular sediment motion and topographic change (Nakagawa & Tsujimoto, 1976; Tsujimoto, 1978; Ancey, 2010; Furbish et al., 2012; Pelosi & Parker, 2014). Considerable attention has been devoted to the problem of discerning the forms of the associated marginal distributions and predicting their parameters or moments under steady, uniform macroscopic flow conditions (Abbott & Francis, 1977; Lajeunesse et al., 2010; Fathel et al., 2015; Furbish, Schmeckle, et al., 2016; Hosseini-Sadabadi et al., 2019; Liu et al., 2019). This objective represents an important step toward the development of models for large-scale fluvial morphodynamics that are consistent with the physics of grain-scale sediment transport.

Likely forms for the marginal probability distributions of particle hop distances and travel times can be obtained from simple assumptions about particle motion through statistical-mechanical arguments (Furbish & Schmeckle, 2013; Furbish, Schmeckle, et al., 2016). These authors suggest that travel times are exponentially distributed while streamwise and absolute lateral hop distances follow a Weibull distribution with shape parameter $0.5 \leq k < 1$, neglecting the small fraction of particles that move in the upstream direction. Previous experimental measurements of particle motion confirm these predictions for uniform flow conditions over a flat streambed (Lajeunesse et al., 2010; Fathel et al., 2015; Campagnol et al., 2015; Furbish, Schmeckle, et al., 2016; Liu et al., 2019; Wu et al., 2020). This still leaves a gap in understanding for the wide range of conditions under which the coupled motion of fluid and sediment amplifies small perturbations in bed elevation leading to the development of ripples and dunes (Van den Berg & Van Gelder, 1993; Southard & Boguchwal, 1990; García, 2008). We therefore seek to determine the forms of these distributions in the presence of equilibrium mobile bedforms.

The processes governing growth, coarsening, and subsequent dynamical behavior of bedforms involve a continual feedback between topography, flow, and sediment transport (Southard & Dingler, 1971; Costello, 1974; McLean, 1990; Best, 1992; Mclean et al., 1994; Venditti et al., 2005a, 2006; Coleman et al., 2006; Coleman & Nikora, 2011; Charru et al., 2013). A rich literature related to flow over bedforms reveals persistent zones of flow acceleration, expansion, and separation which modulate the bed stress and transport fields (McLean et al., 1994; Maddux, Nelson, & McLean, 2003; Maddux, McLean, & Nelson, 2003; Best, 2005, 2009; Muste et al., 2016; Kwoil et al., 2017; Naqshband et al., 2017). Only recently have researchers begun to examine the effects of this interaction on particle kinematics through particle tracking and acoustic techniques. Experimental results indicate that instantaneous quantities like particle activity and velocity vary systematically in relation to topographic position while retaining probability distributions similar to those observed under plane-bed conditions (Wilson & Hay, 2016;

67 Leary & Schmeeckle, 2017; Tsubaki et al., 2018; Terwisscha van Scheltinga et al., 2019).
 68 What remains unclear is how bedforms influence Lagrangian integral quantities like par-
 69 ticle hop distance and travel time, particularly insofar as they relate to the ensemble av-
 70 erage flux and its advective and diffusive components (Furbish et al., 2012; Ancey et al.,
 71 2015).

72 The purpose of this paper is to clarify how bedforms influence time-integrated par-
 73 ticle behavior by comparing observations of particle motion over bedforms and plane-
 74 bed topography. We consider intermediate-timescale hops, defined as periods of contin-
 75 uous motion separated by periods of rest (*sensu* Nikora et al., 2001; Ballio et al., 2018).
 76 Here, we present the results of experiments designed to reveal differences in the prob-
 77 ability distributions of particle hop distance and travel time over equilibrium mobile bed-
 78 forms compared with plane-bed topography. We focus on properties that are relevant
 79 to macroscopic transport to determine whether existing theory developed for plane-bed
 80 topography provides a suitable description of particle motion when bedforms are present
 81 on the bed.

82 2 Theory

83 The topography of a granular bed evolves through the processes of particle entrain-
 84 ment and disentrainment. Each entrainment or disentrainment event produces a small
 85 change in bed elevation which, averaged over time, results in macroscopic topographic
 86 change. This notion underlies the entrainment form of Exner equation (Nakagawa & Tsu-
 87 jimoto, 1976; Tsujimoto, 1978; Parker et al., 2000; Furbish et al., 2012), expressing the
 88 time rate of change of bed elevation η (L) at time t , streamwise position x and cross-stream
 89 position y in terms of the difference between the volumetric particle entrainment rate
 90 E (LT^{-1}) and disentrainment rate D (LT^{-1}) per unit bed area:

$$c_b \frac{\partial \eta}{\partial t}(t, x, y) = -E(t, x, y) + D(t, x, y). \quad (1)$$

91 Here, c_b (-) is the concentration of particles in the bed.

92 Paired entrainment and disentrainment events are explicitly linked through the mo-
 93 tion of individual particles, defining a spatiotemporal displacement vector with compo-
 94 nents of streamwise hop distance L_x (L), lateral hop distance L_y (L), and travel time
 95 T_p (T). Because these quantities are defined in terms of particle exchanges with the bed,
 96 they also form the basis for the relationship between sediment transport and topographic
 97 change. This statement can be demonstrated by invoking a master equation to rewrite
 98 $D(t, x, y)$ as

$$D(t, x, y) = \int_{-\infty}^{\infty} \int_{-\infty}^{\infty} \int_0^{\infty} E(t - T_p, x - L_x, y - L_y) f_{T_p, L_x, L_y}(T_p, L_x, L_y; t - T_p, x - L_x, y - L_y) dT_p dL_x dL_y, \quad (2)$$

99 where $f_{T_p, L_x, L_y}(T_p, L_x, L_y; t, x, y)$ is the joint probability distribution of streamwise hop
 100 distance, lateral hop distance, and travel time of particles entrained at (t, x, y) . Equa-
 101 tion (2) (Furbish et al., 2012) is fundamentally nonlocal in that it integrates conditions
 102 over space and time, however it can be approximated in terms of local variables as a Fokker-
 103 Planck equation (Furbish et al., 2012, 2017), given by

$$c_b \frac{\partial \eta}{\partial t}(t, x, y) = -\frac{\partial}{\partial x} E \overline{L_x} - \frac{\partial}{\partial y} E \overline{L_y} - \frac{\partial}{\partial t} E \overline{T_p} + \frac{1}{2} \frac{\partial^2}{\partial x^2} E \overline{L_x^2} + \frac{1}{2} \frac{\partial^2}{\partial y^2} E \overline{L_y^2} + \frac{1}{2} \frac{\partial^2}{\partial x \partial y} E \overline{L_x L_y} \quad (3)$$

104 where overbars denote ensemble averages. This approximation is valid as long as the marginal
 105 probability distributions of hop distance and travel time have finite first and second mo-
 106 ments and as long as the spatiotemporal scales of particle motion are small relative to

107 the scales of change in flow conditions (Furbish et al., 2012). The one dimensional fluxes
 108 q_x (L^2T^{-1}) and q_y (L^2T^{-1}) are obtained from (3) by assuming conditions are approx-
 109 imately steady in time and uniform in one spatial dimension. These assumptions are ap-
 110 propriate for many practical problems (Furbish et al., 2012; Furbish, Fathel, & Schmeeckle,
 111 2016). Noting that the variance is equal to the mean squared hop distance minus the squared
 112 mean, (i.e. $\sigma_{L_x}^2 = \overline{L_x^2} - \overline{L_x}^2$), the one dimensional fluxes are given by

$$q_x(t, x, y) = E\overline{L_x} - \frac{1}{2} \frac{\partial}{\partial x} E\overline{L_x}^2 - \frac{1}{2} \frac{\partial}{\partial x} E\sigma_{L_x}^2 \quad (4)$$

113 and

$$q_y(t, x, y) = E\overline{L_y} - \frac{1}{2} \frac{\partial}{\partial y} E\overline{L_y}^2 - \frac{1}{2} \frac{\partial}{\partial y} E\sigma_{L_y}^2. \quad (5)$$

114 As noted by Furbish et al. (2017), these terms do not map directly onto conventional ad-
 115 vective and diffusive components of the flux containing the mean particle velocity and
 116 diffusivity. Instead, the first two terms comprise an advective-like flux consisting of a lo-
 117 cal term that is equal to the total flux under uniform transport conditions and a non-
 118 local term that accounts for spatial variability in particle entrainment rate and mean hop
 119 distance. The third term is like a diffusive flux in that it is driven by the variance in par-
 120 ticle hop distance. This interpretation differs from previous studies, reflecting the de-
 121 composition of the raw variance (i.e. $\overline{L_x^2}$) into terms containing the squared mean and
 122 variance. Under this interpretation, the squared coefficient of variation (the ratio of the
 123 standard deviation to the mean) of particle hop distances is like an inverse Peclet num-
 124 ber in that it scales the relative propensity for diffusion-like and advection-like transport.
 125 Similarly, the ratio of the variance to the mean is like a diffusion length in that it scales
 126 the diffusive-like flux in the presence of gradients in the advective-like flux. This idea is
 127 fully discussed in Section 4.4.

128 The objective of this paper is to reveal the manner in which bedforms influence the
 129 marginal probability distribution of particle travel time $f_{T_p}(T_p)$, streamwise hop distance
 130 $f_{L_x}(L_x)$ and lateral hop distance $f_{L_y}(L_y)$. This work is primarily motivated by macro-
 131 scopic morphodynamic modeling problems (e.g., Abramian et al., 2019) for which the
 132 most important features of these distributions are the statistical moments contained in
 133 Equations (3), (4) and (5). We consider multiple indicators of distribution fit, however
 134 we place special emphasis on those which pertain to the estimation of these moments.
 135 Results are interpreted in the context of probability distribution models proposed by Fathel
 136 et al. (2015) which are consistent with various mechanical constraints (Furbish, Schmeeckle,
 137 et al., 2016) as well as with empirical constraints imposed by an extensive dataset of par-
 138 ticle motion over plane-bed topography (Roseberry et al., 2012). These distributions exist
 139 on the domain from zero to infinity and thus ignore hops in the upstream direction.
 140 They also have thin tails and fixed coefficients of variation, implying that the propen-
 141 sity for diffusion-like transport varies in proportion to the advective component of flux
 142 across a wide range of conditions as discussed in more detail below. We aim to deter-
 143 mine the extent to which the constraints that derive from the forms of these distribu-
 144 tions provide a realistic foundation for modeling macroscopic sediment transport phen-
 145 nomena when bedforms are present.

146 3 Experiments

147 3.1 Overview

148 In order to compare the ensemble statistics of particle motions that are character-
 149 istic of plane-bed and bedform topography, we conducted two flume experiments differ-
 150 entiated primarily by the presence or absence of equilibrium bedforms. For each exper-
 151 iment we recorded videos of fluorescent tracer particles that were used to construct em-
 152 pirical distributions of particle hop distance and travel time. In considering fixed dis-
 153 tributions of these quantities, we appeal to the idea of an ensemble of nominally iden-

154 tical systems first described by Gibbs (1902) and elaborated recently with respect to bed-
 155 load transport by Furbish et al. (2012). We designed our experiments so that the dis-
 156 tributions measured over a finite temporal and spatial domain may be assumed to be
 157 equivalent to the instantaneous ensemble distribution at any position and time. This as-
 158 sumption is reasonable as long as the macroscopic average conditions are steady and uni-
 159 form over the domain of data collection.

160 Theory and analyses presented here assume a steady, uniform probability distri-
 161 bution of particle hop distance and travel time that is independent of x , y and t . Although
 162 previous studies find that particle motion depends on location relative to bedform fea-
 163 tures (Wilson & Hay, 2016; Leary & Schmeeckle, 2017; Tsubaki et al., 2018; Terwisscha
 164 van Scheltinga et al., 2019), we emphasize that the existence of bedforms does not pre-
 165 clude the possibility of considering a stationary distribution averaged over all possible
 166 configurations of bedform topography. Bedforms are viewed as stochastic fluctuations
 167 in bed elevation, and there is a timescale over which a single location on the bed expe-
 168 riences a representative sample of all possible configurations of topography character-
 169 istic of the macroscopic flow conditions (e.g. the bedform field timescale as envisioned
 170 by Furbish et al., 2012). In this context, the term "macroscopic" implies averaging over
 171 scales much larger than an individual bedform.

172 In order to ensure that measured distributions reflect ensemble probability distri-
 173 butions characteristic of macroscopic flow conditions, measured particle motions would
 174 ideally contain a sample that is representative of all possible microconfigurations of flow
 175 and topography. In practice, this means that particle hops should be measured over spa-
 176 tiotemporal scales that are much larger than those of significant autocorrelation in flow
 177 velocity and bed elevation. Due to practical limitations, this was not possible for the bed-
 178 form condition: particle motions were recorded over a small region of the bed with stream-
 179 wise and cross-stream dimensions comparable to the bedform lengthscale which we as-
 180 sume is similar to the autocorrelation lengthscale of topography (Nordin, 1971; Nikora
 181 et al., 1997). Nonetheless, we posit that these data are sufficient to reveal important fea-
 182 tures of particle motion over bedforms. We report distributions sampling hops originat-
 183 ing on both stoss and lee regions of a single bedform over two ten second intervals. All
 184 tracer particle motions in the measurement window were included in our analysis such
 185 that the empirical distributions approximately reflect the relative entrainment rates in
 186 stoss and lee regions of one bedform. For additional discussion of issues related to the
 187 finite sampling window, see Section 4.5.

188 3.2 Description of Experiments

189 Experiments were conducted in a 7.2 m long \times 0.29 m wide flume capable of re-
 190 circulating both sediment and water. Bedforms were allowed to develop under constant
 191 flow conditions over a period of 48 hours, at which point particle motions were recorded
 192 using a downward-looking camera. Plane-bed conditions were then achieved by manu-
 193 ally grading the bed using a plastic paddle, and particle motions were recorded again.
 194 Flume boundary conditions remained constant throughout this procedure: water discharge
 195 was 18 L/s, the flume slope was 0.001, and flow depth at the outlet was set to approx-
 196 imately $H = 0.16$ m. The mean flow velocity was $U = 0.39$ m/s, and the Froude num-
 197 ber was $Fr = U/\sqrt{gH} = 0.31$.

198 The bed material consisted of natural sediment collected in an aeolian dune field
 199 near the Seminole Reservoir in Wyoming. Fine sediment was removed prior to these ex-
 200 periments by continuously siphoning turbid water in the outlet reservoir and replacing
 201 it with clear water. The resulting bed material had a median diameter of 330 μm and
 202 median settling velocity $\omega_s = 4.4$ cm/s. The base-2 logarithmic standard deviation was
 203 0.69 (68% of the bed material was within a multiplicative factor of $2^{0.69} = 1.61$ of the
 204 mean). This is typical of hydraulically sorted natural sediment in fluvial systems, but

is a significant departure from the single-grain size experiments reported in previous studies. The implications of this difference are discussed in Section 4.2.

Particle motions were measured using videos of fluorescent tracer particles. To this end, a small fraction of the bed material was removed from the flume and coated with a thin layer of fluorescent paint. Although we cannot rule out the possibility that the paint caused small differences in particle properties, we expect that such effects are small and do not influence the primary findings of this study. Approximately 30 cm^3 (including pore space) of tracer particles were added back into the flume and allowed to mix with the unpainted bed material over a period of several weeks of continuous run time under a range of flow conditions. The thickness of sediment within the flume was approximately 8 cm such that the total volume of sediment in the flume including pore space was approximately 170000 cm^3 and tracer particles composed an estimated 0.017 % of the bed material. For comparison, the tracer particle percentage estimated by comparing the tracer particle flux and the bedform bedload flux (discussed below) is 0.019 %. Particles were illuminated with black lights (GE Black Light Blue bulbs, peak wavelength = 368 nm) through the side windows of the flume test reach (Figure 1a, 1b), which increased the contrast of tracer particles against the bed and facilitated consistent tracking (Naqshband et al., 2017). We assume this procedure provides an unbiased sample of complete particle hops representing the full distribution of particle sizes.

Acoustic measurements of the near-bed flow velocity profile were collected over equilibrium bedforms to compute the bed stress condition (Bagherimiyab & Lemmin, 2013; Le Bouteiller & Venditti, 2015). The sidewall-corrected shear velocity was $u_* = 2.4 \text{ cm/s}$. This produced bedload dominated bedforms with a suspension number (the ratio of shear velocity to sediment settling velocity) of 0.54. For comparison, the unit bedload flux estimated from bedform migration using the bedform bedload equation of Simons et al. (1965) was $q_b = 4.1 \times 10^{-7} \text{ m}^2/\text{s}$. Applying the Wong and Parker (2006) bedload equation and solving for stress suggests that the effective shear velocity (i.e. skin friction) driving sediment transport was $u_{*sk} = 1.8 \text{ cm/s}$. This is consistent with the notion that pressure differences across a bedform reduce the bedload transport rate associated with a specified average bed stress.

Although fluid velocities were not measured directly for the plane-bed condition, we may estimate of the shear velocity by comparing the relative magnitudes of the tracer particle flux (discussed below) using the Wong and Parker (2006) bedload equation. The tracer particle flux for the plane-bed experiment was 2.1 particles per second per meter width. The bedload flux is estimated to be $1.9 \times 10^{-7} \text{ m}^2/\text{s}$ leading to an estimated shear velocity of $u_* = 1.7 \text{ cm/s}$ and a suspension number of 0.38. We emphasize that this estimate requires substantial assumptions and is reported here as a rough approximation to contextualize our experiments. However, the specific values of the shear velocity are not central to any of the theoretical developments or interpretations presented below.

Characteristic scales of bedform topography were computed from one-dimensional scans obtained using an ultrasonic profiler mounted to a moving cart. Equilibrium bedforms had a characteristic height $H_c = 1.5 \text{ cm}$, a characteristic length $L_c = 16 \text{ cm}$, and a characteristic migration velocity $V_c = 0.50 \text{ cm/minute}$. Bedform height was determined using $H_c = 2\sqrt{2}\sigma_\eta$ where σ_η is the standard deviation of bed elevation (McElroy, 2009). L_c was determined from the spectral centroid of the bed profile and V_c was determined from the maximum of the cross-correlation function of successive scans (Van der Mark & Blom, 2007). The characteristic evolution timescale of bed elevation η computed as $T_\eta = \eta/(\partial\eta/\partial t)$, was approximately 8 minutes, such that topography is effectively fixed within the ten-second data collection intervals.

Videos of particle motion were recorded using a submerged downward-looking camera mounted near the centerline of the flume with the lens approximately 15 centime-

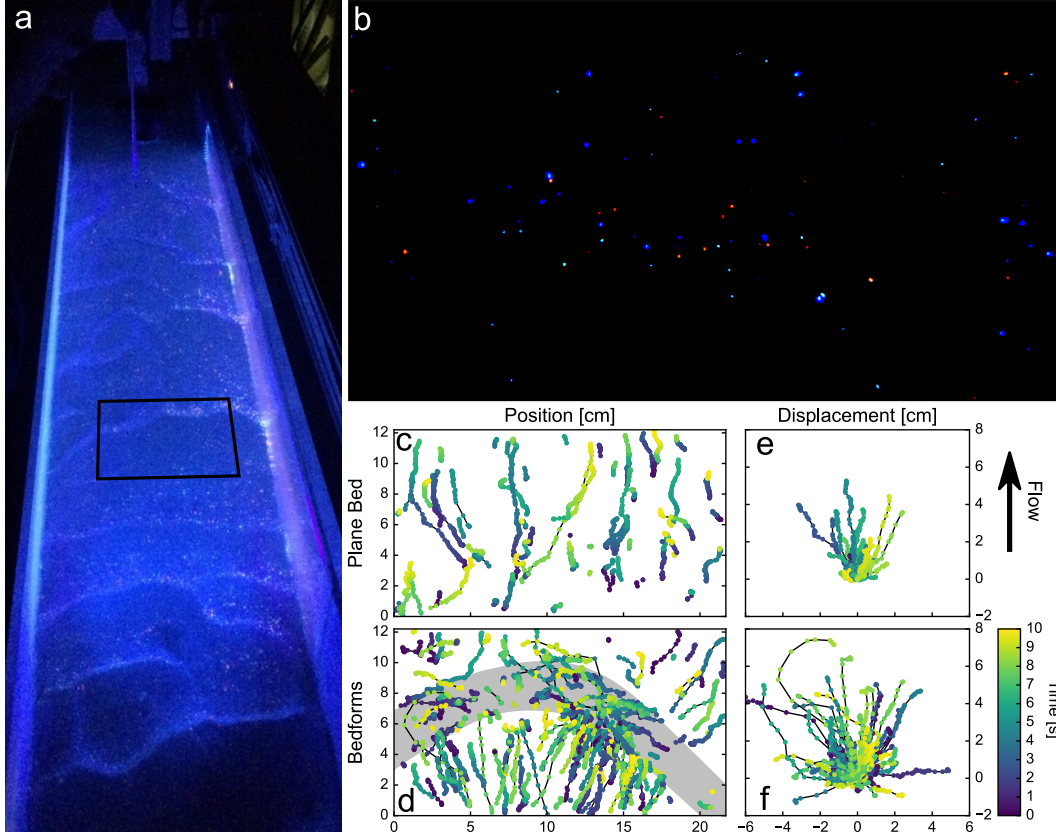


Figure 1. Experimental setup and tracked particle motions. (a) Oblique view of flume with bedforms. Black box indicates the approximate region of the bed where videos of fluorescent tracer particles were recorded. (b) Still image from video of fluorescent tracer particles during the bedform condition. Flow is from bottom to top. (c) Tracked particle motions over plane-bed and (d) bedform topography. Grey region in (d) indicates the position of a bedform lee face. Note that the particle transport direction exhibits conditional dependence on topographic configuration in the vicinity of the particle that is discussed in more detail in section 4.1. (e) Visualization of particle displacements over plane-bed and (f) bedform topography. Topographic effects manifest as qualitative differences in between (e) and (f).

257 ters from the bed. Videos were collected at a resolution of 1920 by 1080 pixels and at
 258 a frame rate of 30 frames per second. This window covered a streamwise distance of 12.2
 259 cm, and a cross-stream distance of 21.7 cm. Two ten-second intervals from each video
 260 were used for this analysis. Image registration and rectification were performed using
 261 OpenCV in Python (Bradski, 2000) Particles were digitized manually using TrackMate
 262 (Tinevez et al., 2017), an open-source particle tracking package for ImageJ (Schindelin
 263 et al., 2012; Rueden et al., 2017). All particles that moved during each interval were tracked
 264 for their entire visible path, including rest times (Figure 1).

265 The position of the particle centroid was tracked to within roughly one pixel such
 266 that the total uncertainty in each estimate of particle hop distance is roughly 0.022 cm
 267 (or one pixel at the start and beginning of each hop). Note that this is comparable to
 268 the median particle diameter. The uncertainty in each particle hop distance is approx-
 269 imately 6.25% of the mean hop distance in the plane-bed experiment and 9.5% of the
 270 mean hop distance in the bedform experiment. This error may be positive or negative

271 such that it is unlikely to bias estimates of the mean hop distance. In principle, this type
 272 of uncertainty could result in a positive bias in estimates of the variance by adding nor-
 273 mally distributed noise, however the magnitude of this effect is small and equivalent for
 274 both experiments. As a result, it is ignored in the analysis presented below.

275 The timing of the end and beginning of particle motions can be constrained to within
 276 one frame (0.033 s). Assuming perfect detection of particle motion, the measured hop
 277 duration will always be greater than or equal to the true hop duration because motion
 278 will always be registered as starting the frame before motion begins and ending the frame
 279 after motion ends. This effect will introduces a positive bias to empirical estimates of
 280 the mean travel time if the particle is assumed to be moving for the full duration over
 281 which motion is observed. Correcting for this bias is not trivial and depends on assump-
 282 tions about the underlying distribution of particle travel times, however we note that the
 283 effect on the computed moments is small, biasing the estimate of the mean travel time
 284 by approximately one frame time and introducing essentially no bias to the estimate of
 285 the variance. A moderate bias correction does not influence the primary findings of this
 286 paper and is not performed here.

287 **3.3 Definition of a Particle Hop**

288 The concept of a complete particle “hop” follows from the notion that particles may
 289 occupy one of two mutually exclusive states: motion and rest (Hosseini-Sadabadi et al.,
 290 2019). This distinction is critical to the interpretation of particle-kinematic statements
 291 of sediment mass conservation, namely, the divergence and entrainment forms of the Exner
 292 equation. However, differentiating between active and stationary particles is not straight-
 293 forward: grains on the bed surface may wiggle in place without moving appreciably and
 294 may accumulate significant displacements over long timescales due to granular creep (Houssais
 295 et al., 2015). In fact, granular transport occurs via numerous phases (Houssais & Jerol-
 296 mack, 2017); the binary view of mobility is merely a convenience adopted to delineate
 297 highly disparate scales of particle velocity and flux for the purposes of mathematical ab-
 298 straction.

299 This reasoning suggests that particles on or below the bed surface are not truly sta-
 300 tionary in the sense that they have detectable mean velocities averaged over long timescales.
 301 Consequently, empirical studies of particle motion which attempt to differentiate between
 302 mobile and immobile grains do so according to criteria that, despite their intuitive ap-
 303 peal, lack clear physical justification (Hosseini-Sadabadi et al., 2019). For example, par-
 304 ticles are often treated as mobile when their velocity exceeds a threshold value that is
 305 either explicitly stated or set implicitly by the resolution of the technique used to dig-
 306 itize particle motions. Such criteria retain the important property of mass conservation
 307 as long as the mobile and immobile states encompass all grains and are mutually exclu-
 308 sive, and mobile particles are not counted towards the elevation of the bed. Moreover,
 309 velocity criteria are valid in scenarios where sediment transport and morphodynamics
 310 are dominated by bedload transport rather than granular creep.

311 Other criteria that are equally valid from a theoretical perspective may lead to dif-
 312 ferent results as to whether certain particles are mobile or immobile, ultimately produc-
 313 ing differences in measured distributions of particle hop distance and travel time (Hosseini-
 314 Sadabadi et al., 2019). We recognize this issue but do not attempt to solve it here. In-
 315 stead, we use an approach that is similar to previous studies (Liu et al., 2019) and ac-
 316 knowledge where our results might be sensitive to this choice. Velocity criteria are an
 317 objective, reproducible solution to this problem. Different velocity thresholds may pro-
 318 duce different distributions of particle hop distance and travel time but will lead to es-
 319 sentially the same estimate of the macroscopic flux as long as the velocity threshold is
 320 sufficiently small.

Table 1. Summary Statistics

	Plane Bed	Bedforms
Mean travel time $\overline{T_p}$	0.18 s	0.13 s
Variance $\sigma_{T_p}^2$	0.042 s ²	0.023 s ²
Coefficient of variation $\sigma_{T_p}/\overline{T_p}$	1.13	1.13
Mean streamwise hop distance $\overline{L_x}$	0.32 cm	0.21 cm
Variance $\sigma_{L_x}^2$	0.43 cm ²	0.47 cm ²
Coefficient of variation $\sigma_{L_x}/\overline{L_x}$	2.04	3.25
Streamwise diffusion length ℓ_{D_x}	1.34 cm	2.22 cm
Inverse Peclet number Pe_x^{-1}	4.2	10.6
Mean lateral hop distance $\overline{L_y}$	-2.2×10^{-3} cm	-2.8×10^{-2} cm
Variance $\sigma_{L_y}^2$	0.11 cm ²	0.27 cm ²
CV of absolute values $\sigma_{ L_y }/\overline{ L_y }$	2.20	2.70
Coefficient of lateral transport $\sigma_{L_y}/\overline{L_x}$	1.03	2.49
Lateral diffusion length ℓ_{D_y}	0.34 cm	1.29 cm
Inverse Peclet number Pe_y^{-1}	1.07	6.17

321 The exact value of the velocity threshold used here was chosen following the ap-
322 proach of Liu et al. (2019). Specifically, we examined particle motions under a range of
323 velocity thresholds and found that values ranging from 0.2 cm/s to 0.5 cm/s reliably dis-
324 criminated between visually-identified mobile and immobile states. The exact value of
325 the threshold within this range affects the absolute magnitude of empirical moments but
326 has almost no effect on the primary findings of this paper which concern their relative
327 magnitudes and the shape of the distribution functions. Reported results were obtained
328 using a velocity threshold of 0.3 cm/s. This value is significantly lower than the thresh-
329 old velocities adopted by Liu et al. (2019) and Lajeunesse et al. (2010), perhaps because
330 the lower frame rate (30 frames per second in the present study compared with 90 frames
331 per second) allows more precise estimates of frame-averaged velocity. This number cor-
332 responds to a one-frame displacement of 0.01 cm over $1/30^{th}$ of a second, which is roughly
333 one pixel or one third of the median grain diameter. Particles with frame-averaged ve-
334 locities greater than or equal to the threshold velocity are considered mobile, and all other
335 particles are considered immobile. A complete hop is defined as an uninterrupted period
336 in the mobile state that begins and ends with transitions to and from the immobile state.
337 Insofar as previous plane-bed studies necessarily employ some variant of this approach,
338 it is sufficient to reveal the extent to which particle motions over bedforms conform to
339 existing theory.

340 4 Results and Discussion

341 The experimental procedure described in the previous section yielded measurements
342 of 360 complete particle hops for the plane bed condition and 1170 hops for the bedform
343 condition. These data are visualized in Figure 1, which shows all tracked particle motions,
344 and Figure 2, which shows the pairwise relationships between variables. Descriptive
345 statistics are reported in Table (1).

346 Tracked particle paths reveal significant qualitative differences between the plane-
347 bed and bedform experiments. Notably, particle behavior clearly depends on position
348 relative to bedform features in a manner that is reminiscent of the backward facing step
349 experiments of Leary and Schmeckle (2017) and the particle velocity fields reported by
350 Tsubaki et al. (2018) and Terwisscha van Scheltinga et al. (2019). Particle transport di-

351 rection is highly variable in the region of flow separation immediately downstream of the
 352 bedform crest. On the stoss side, particle transport direction is more regular and the mean
 353 local transport direction is approximately perpendicular to the nearest crest (Figures 1c,
 354 1d). These behaviors produce significant qualitative differences in the characteristics of
 355 particle displacement as shown in figures 1e, 1f, and 2.

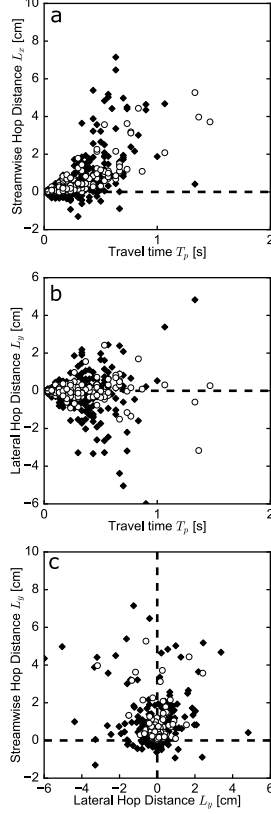


Figure 2. Pairwise comparison of measured particle hop distances and travel times. Dashed lines indicate particle hop distances of zero. Bedform data are shown in black diamonds and plane-bed data are shown in white circles. Panels (a) and (b) illustrate a conditional dependence of streamwise and lateral particle hop distance on travel time that is used by Fathel et al. (2015) to derive the Weibull distribution for particle hop distances. Panel (c) encompasses the primary qualitative differences between the plane-bed and bedform experiments; particle motions over bedforms exhibit a wider spread in both the streamwise and cross-stream directions, and upstream hops appear to occur more frequently and have larger magnitudes over bedforms than over planar topography.

356 Empirical moments are reported in Table 1. Although the mean particle travel time
 357 and mean streamwise hop distance are slightly larger in the plane-bed experiment, we
 358 find that the distribution of particle hop distances over bedforms has much larger vari-
 359 ance in the cross-stream and streamwise directions. This difference reflects the increased
 360 variability in hop distances evident in Figure 2. The sample size in both experiments was
 361 sufficiently large such that conventional measures of statistical uncertainty indicate that
 362 moments are estimated with high precision. For example, the 95% asymptotic confidence
 363 interval for the estimate of the mean travel time in the bedform experiment ranges from
 364 0.12 s to 0.14 s. More sophisticated estimates of statistical uncertainty produce similar
 365 results. However, these statistical measures only quantify uncertainty associated with

366 measurement error and finite sample size, and cannot quantify uncertainty associated
 367 with the finite measurement window (Section 4.5). We believe this effect is the primary
 368 source of uncertainty in our results. Due to the systematic misrepresentation of true un-
 369 certainty, confidence intervals for other parameters are not reported here.

370 4.1 Physical Mechanism for Observed Differences in Particle Behavior

371 Previous studies of particle motion find that particle velocities are conditionally
 372 dependent on the local topographic configuration due to the coupling of topography, flow,
 373 and sediment transport (Tsubaki et al., 2018; Terwisscha van Scheltinga et al., 2019).
 374 Topographically-induced correlations in flow velocity exist over spatial scales that are
 375 comparable to the bedform length; in contrast, we find that the average hop distance is
 376 much smaller than a bedform length. As a result, individual particle hops do not con-
 377 verge on the ensemble statistics of motion (Fathel et al., 2016; Furbish et al., 2017), in-
 378 stead reflecting topographically-induced deviations from the mean flow field.

379 As an example, consider a particle that is entrained on a stoss slope that is oriented
 380 obliquely relative to the mean flow direction. This topographic configuration usually re-
 381 sults in flow being redirected laterally (Best, 2005; Venditti et al., 2005b), causing a cor-
 382 responding lateral component of sediment movement (Tsubaki et al., 2018; Terwisscha
 383 van Scheltinga et al., 2019) that is possibly amplified by gravitational effects (Parker et
 384 al., 2003). Because particle motions are short relative to the spatial scales of topogra-
 385 phy, this particle is likely to spend the entire interval from entrainment to disen-
 386 trainment on this oblique slope. A large lateral hop distance would be highly improbable over
 387 plane-bed topography under similar mean flow conditions, but would be typical for par-
 388 ticles entrained in this location.

389 We suggest that observed differences in probability distributions of particle hop dis-
 390 tance and travel time are the result of this effect. Over plane-bed topography, turbulent
 391 fluctuations in flow velocity and collisions between particles are the primary sources of
 392 variability (Nikora et al., 2001, 2002; Seizilles et al., 2014; Fathel et al., 2015; Hosseini-
 393 Sadabadi et al., 2019). We infer that localized fluctuations in flow velocity driven by bed-
 394 form topography cause variability in particle behavior that is superimposed on variabil-
 395 ity driven by turbulence and particle collisions. Tsubaki et al. (2018) and Terwisscha van
 396 Scheltinga et al. (2019) report similar behaviors, which manifest as deviations from the
 397 mean particle velocity field characterized by crest-normal transport on the stoss sides
 398 of bedforms (Fryberger & Dean, 1979; Werner & Kocurek, 1997), and highly variable trans-
 399 port over lee faces and troughs (figures 1c, 1d). This causes a marked qualitative differ-
 400 ence in particle behavior that is apparent in Figures 1e, 1f, and 2 as enhanced variabil-
 401 ity in transport direction and distance. Quantitative analyses presented below contex-
 402 tualize these observations in terms of the entrainment forms of the flux and Exner equa-
 403 tions.

404 4.2 Effect of Naturally Sorted Sediment

405 Our analysis assumes that the marginal distributions of particle hop distance and
 406 travel time have thin tails such that the mean and the variance are well defined. Although
 407 previous studies suggest that this is true for monodisperse sediment undergoing low bed-
 408 load transport (Fathel et al., 2015; Furbish, Schmeckle, et al., 2016; Liu et al., 2019),
 409 heavy-tailed distributions of hop distance and travel time are possible if a range of grain
 410 sizes are present and the mean hop distance varies with grain size (Ganti et al., 2010).
 411 Our experiments involved naturally sorted sediment which is valuable insofar as we seek
 412 to understand natural transport systems. However, it is important to consider the ex-
 413 tent to which theory developed for uniform sediment may be applicable to the present
 414 research.

415 As a starting point, we consider the distribution of streamwise hop distance as a
 416 margin of the joint distribution of particle hop distance and grain size, $f_{L_x, D}(L_x, D)$:

$$f_{L_x}(L_x) = \int_0^{\infty} f_{L_x|D}(L_x|D) f_D(D) dD. \quad (6)$$

417 Ganti et al. (2010) clarify how this integration may lead to a heavy-tailed distribution
 418 of hop distance. Specifically, if $f_{L_x|D}(L_x|D)$ is exponential with mean varying in pro-
 419 portion (or inverse proportion) to grain size and $f_D(D)$ is a Gamma distribution with
 420 shape parameter α , then $f_{L_x}(L_x)$ is a generalized Pareto distribution. This argument
 421 also holds for particle travel times. In this scenario, the mean only converges if $\alpha > 1$
 422 and the variance only converges if $\alpha > 2$. We note that the the coefficient of variation
 423 of a Gamma distribution is equal to $1/\sqrt{\alpha}$. Thus, the weight of the tails depends on the
 424 degree of sorting of the bed material, where well sorted sediments are less likely to have
 425 heavy-tailed distributions of hop distance and travel time. The best-fit Gamma distri-
 426 bution for the bed material used in these experiments has a shape parameter $\alpha = 4.83$
 427 such the mean and variance are well-defined. On this basis, we suggest that it is reason-
 428 able to expect that the distributions of hop distance and travel time are thin-tailed.

429 Even if the distributions have thin tails, variability in grain size implies that the
 430 marginal probability distributions of hop distance and travel time depend on (a) the func-
 431 tional form of the grain-size specific distribution of hop distance and travel time (e.g. $f_{L_x|D}(L_x|D)$),
 432 (b) the relationship between the grain size and the parameters of this conditional dis-
 433 tribution, and (c) the relative entrainment rates of different grain sizes (which may dif-
 434 fer from the grain size distribution of the bed material due to selective entrainment and
 435 vertical sorting). Each of these effects may be present in our data, however we focus on
 436 the collective outcome and have not attempted to evaluate their importance individu-
 437 ally.

438 4.3 Comparison of Theoretical and Empirical Distributions

439 4.3.1 Travel Times

440 Previous studies suggest that the marginal probability distribution of bedload par-
 441 ticle travel times is exponential (Fathel et al., 2015; Furbish, Schmeckle, et al., 2016),
 442 i.e.:

$$f_{T_p}(T_p) = \frac{1}{\tau} e^{-T_p/\tau}, \quad (7)$$

443 where τ is a characteristic travel time. This implies a fixed temporal disen-
 444 trainment rate for moving particles (Tucker & Bradley, 2010; Furbish, Schmeckle, et al., 2016). In other
 445 words, the probability that a particle in motion at time t is deposited over the next small
 446 time interval dt does not depend on how long the particle has been in motion at t in the
 447 absence of other information about the flow and topographic configuration. Previous stud-
 448 ies have suggested that this this distribution is not strictly exponential (due to the pres-
 449 ence of truncated tails) but may be treated as such for most practical purposes (Fathel
 450 et al., 2015).

451 Quantile-quantile (Q-Q) plots (figure 3a, 3b) and histograms (figure 3c, 3d) reveal
 452 that the exponential distribution provides a reasonable fit to plane-bed and bedform par-
 453 ticle travel times (Figure 3). The coefficient of variation (the ratio of the standard de-
 454 viation to the mean) of an exponentially distributed random variable is 1, which is an
 455 important diagnostic test of distribution fit. Measured coefficients of variation are 1.13
 456 for both experiments (Table 1). Based on these observations, we suggest that (a) our data
 457 confirm the findings of previous authors with regard to the exponential distribution of
 458 particle travel times over plane-bed topography and (b) the presence of equilibrium mo-
 459 bile bedforms does not substantially influence the functional form of this distribution.
 460 We also find no evidence that the distribution of travel times is heavy-tailed despite vari-
 461 ability in bed material grain size typical of natural fluvial systems.

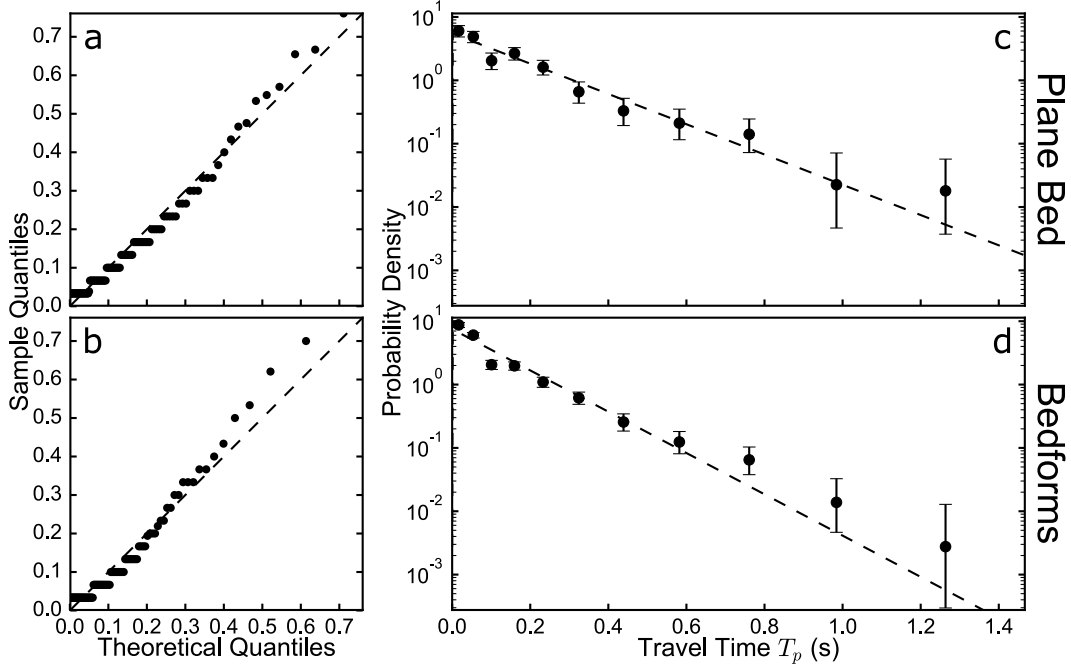


Figure 3. Quantile-quantile (a, b) and density plots (c,d) comparing measured distributions of particle travel time with best-fit exponential distributions (dashed lines). Densities were computed using logarithmically-spaced bins. Error bars represent the 95% Bayesian credible interval for a binomial proportion obtained using Jeffrey’s prior (Brown et al., 2001). Deviations from theory are similar in both experiments and do not cause a substantial difference in the coefficient of variation in travel times. We interpret observed deviations as measurement error rather than as genuine features of the dataset.

462

4.3.2 Streamwise Hop Distances

463

464

465

466

467

468

469

470

471

472

473

474

475

476

477

478

479

480

Theoretical distributions proposed by Fathel et al. (2015) to describe streamwise hop distances follow from exponentially distributed travel times combined with the assumption that particles with longer travel times have the opportunity to attain higher velocities (Roseberry et al., 2012). This suggests that a conditional dependence of particle hop distance on travel time (evident in Figures 2a and 2b) that can be approximated by $L_x = a_x T_p^{b_x} + \epsilon_x$ (Fathel et al., 2015), where a_x is a characteristic acceleration, ϵ_x is a residual deviation term, and b_x is a scaling parameter that may be connected to suspension conditions. For bedload-dominated transport, particle travel times are short relative to the timescale required to accelerate particles to the mean near-bed fluid velocity and particle hops are dominated by the unsteady acceleration and deceleration phases of motion (Campagnol et al., 2015). As a result, previous studies which report bedload-dominated transport over plane-bed topography (e.g., Fathel et al., 2015) find that $L_x/T_p \sim T_p$ and leading to $b_x = 2$. It has been suggested that this dependence disappears at higher suspension conditions (Anczyk & Heyman, 2014; Heyman et al., 2016; Campagnol et al., 2015; Wu et al., 2020), however we restrict our attention to bedload-dominated transport similar to previous plane-bed studies. Ignoring the residual deviation and assuming exponentially distributed travel times leads to the expectation that hop distances follow Weibull distributions (Fathel et al., 2015). Thus, the marginal distribution of stream-

481 wise hop distances is given by

$$f_{L_x}(L_x) = \frac{k_x}{\lambda_x} \left(\frac{x}{\lambda_x} \right)^{k_x-1} e^{-(x/\lambda)^{k_x}} \quad (8)$$

482 where $k_x = 1/b_x$ and $\lambda_x = a_x \tau^{b_x}$. If $k_x = 1/2$, then the mean and variance in particle
 483 hop distance can be expressed in terms of model parameters as $\overline{L_x} = 2a_x \tau^2$ and
 484 $\sigma_{L_x}^2 = 20a_x^2 \tau^4$.

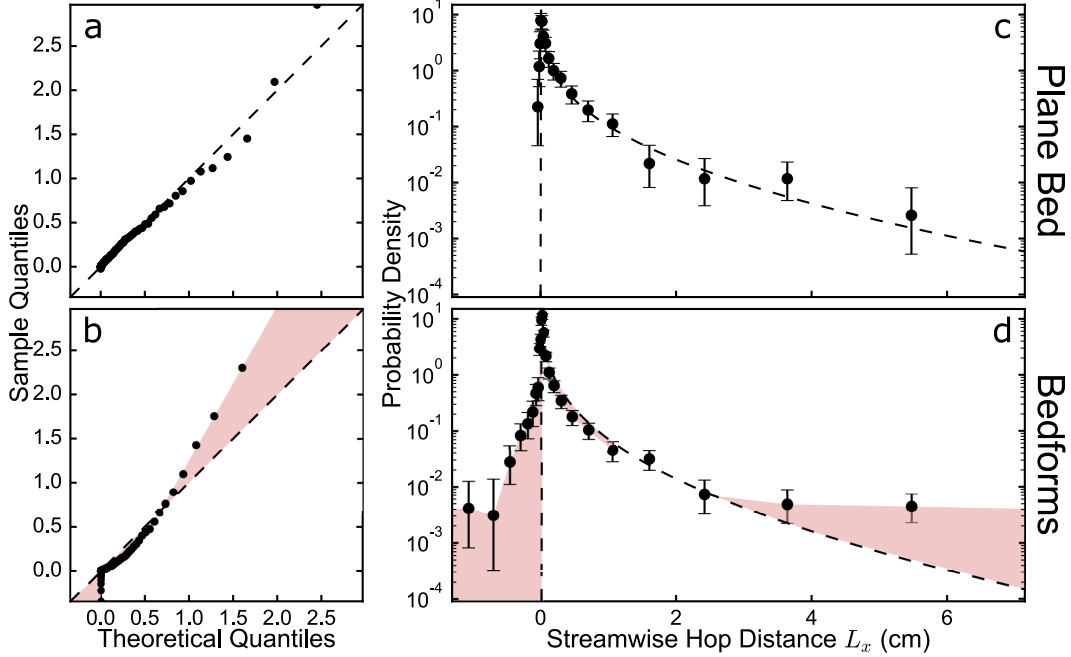


Figure 4. Quantile-quantile (a, b) and density plots (c, d) comparing measured distributions of streamwise hop distance with best-fit Weibull distributions with shape parameter $k = 1/2$ (dashed lines). Densities were computed using logarithmically-spaced bins. Error bars represent the 95% Bayesian credible interval for a binomial proportion obtained using Jeffrey’s prior (Brown et al., 2001). Red regions in panels (b) and (d) highlight systematic deviations from plane-bed theory.

485 In considering whether this distribution is suitable for hop distances over bedforms,
 486 we focus primarily on the considerations relevant to macroscopic morphodynamic mod-
 487 eling outlined in Section 2. Specifically, we ask whether estimates of distribution param-
 488 eters a_x and τ can lead to accurate predictions of the mean hop distance $\overline{L_x}$ and the vari-
 489 ance $\sigma_{L_x}^2$. This question is of central importance if the eventual goal is to construct macro-
 490 scopic morphodynamic models that are consistent with the physics of grain-scale sed-
 491 iment transport. The proposed Weibull distribution with shape parameter $k = 1/2$ pre-
 492 scribes a fixed coefficient of variation $\sqrt{5} \approx 2.23$. This implies that the variance $\sigma_{L_x}^2$
 493 can be estimated from a measurement of the mean. If k is allowed to vary between $1/2$
 494 and 1, the coefficient of variation must be between 1 and $\sqrt{5}$. The coefficient of varia-
 495 tion therefore is an important indicator of distribution fit; if it is significantly larger than
 496 $\sqrt{5}$ or smaller than 1, no single estimate of model parameters appropriately character-
 497 izes the advective and diffusive components of the flux simultaneously.

498 Measured streamwise hop distances in the plane-bed experiment have a coefficient
 499 of variation of 2.05 compared with 2.23 predicted from theory. Ignoring upstream hops

500 does not significantly affect the estimate of the mean because only 5% of hops occur in
 501 the upstream direction and the average upstream hop distance is very small relative to
 502 the average downstream hop distance (0.1 mm compared with 3.5 mm). As with travel
 503 times, we find no evidence that the distribution of particle hop distance is heavy-tailed
 504 for the moderately sorted sand used in this experiment. We suggest suggest that the dis-
 505 tribution of streamwise bedload hop distances over plane-bed topography in hydraulically
 506 sorted, natural sediments can be sufficiently approximated using a Weibull distri-
 507 bution with shape parameter $k = 1/2$ in the context of macroscopic transport prob-
 508 lems.

509 In contrast, the distribution of streamwise hop distances over bedforms exhibits sig-
 510 nificant deviations from theory. Qualitative comparison of the histogram and a best-fit
 511 theoretical distribution (figure 4d) reveals systematic differences in probability density
 512 across the full range of observed hop distances that results in a concave-up relationship
 513 between empirical and theoretical quantiles (Figure 4b). A much larger fraction of hops
 514 occur in the upstream direction (15%) and these possess an average upstream displace-
 515 ment that are a significant fraction of the average downstream displacement (0.8 mm com-
 516 pared with 2.8 mm). We conclude that the presence of bedforms leads to an important
 517 difference in empirical moments: the coefficient of variation in measured streamwise hop
 518 distances is 3.25, meaning that the standard deviation does not vary with the mean as
 519 expected. Instead, observed spatiotemporal correlations between particle behavior and
 520 topography lead to an increased variance relative to the mean (figure 1d, 1f) that vio-
 521 lates constraints imposed by plane-bed theory.

522 **4.3.3 Lateral Hop Distances**

523 The streamwise and lateral coordinates are defined such that lateral hop distances
 524 have a mean of zero and are symmetrically distributed under steady, uniform transport
 525 conditions considered here. Like with streamwise hop distances, Roseberry et al. (2012)
 526 and Fathel et al. (2015) find that the absolute lateral displacement is correlated with travel
 527 time leading to $|L_y| = a_y T_p^{b_y} + \epsilon_y$, where $b_y \approx 2$. The distribution of absolute lateral
 528 hop distances can therefore be approximated using a Weibull distribution with shape pa-
 529 rameter $k = 1/2$ and scale parameter $\lambda = a_y \tau^2$. For particle motions over plane-bed
 530 topography, quantile-quantile (figure 5a) and histogram plots (figure 5c) reveal that ab-
 531 solute lateral hop distances over plane-bed topography are well-approximated by the best-
 532 fit Weibull distribution with fixed shape parameter $k = 1/2$.

533 Once again, we consider whether the proposed Weibull distribution can accurately
 534 quantify the first and second moments of measured lateral hop distances. This distri-
 535 bution implies that the mean absolute lateral hop distance is given by $\overline{|L_y|} = 2a_y \tau^2$,
 536 the variance is given by $\sigma_{|L_y|}^2 = 20a_y^2 \tau^4$, and the coefficient of variation is $\sqrt{5}$. Because
 537 the distribution of signed lateral hop distances is symmetric with mean equal to zero,
 538 the variance is equal to the raw variance of absolute lateral hop distances, i.e. $\sigma_{L_y}^2 =$
 539 $\overline{|L_y|}^2 = \overline{|L_y|}^2 + \sigma_{|L_y|}^2$. The first and second moments that are relevant to macroscopic
 540 transport problems can be expressed in terms of distribution parameters as $\overline{L_y} = 0$ and
 541 $\sigma_{L_y}^2 = 24a_y^2 \tau^4$.

542 The empirical coefficient of variation for absolute lateral hop distances is 2.20, com-
 543 pared with 2.23 predicted from theory. For particle motions over bedform topography,
 544 the coefficient of variation in absolute lateral hop distances is 2.7, while the histogram
 545 plot (figure 5d) reveals systematic deviations from predicted bin frequencies resulting
 546 in a concave-up relationship between theoretical and measured quantiles (figure 5b). Again,
 547 this may indicate a heavy-tailed distribution of absolute lateral hop distances. If the dis-
 548 tribution is not heavy tailed, then bedforms cause a significant increase in the variance
 549 of the signed lateral hop distances (0.27 cm² compared with 0.11 cm²), both by alter-
 550 ing the shape of the distribution of absolute lateral hop distances and by increasing the

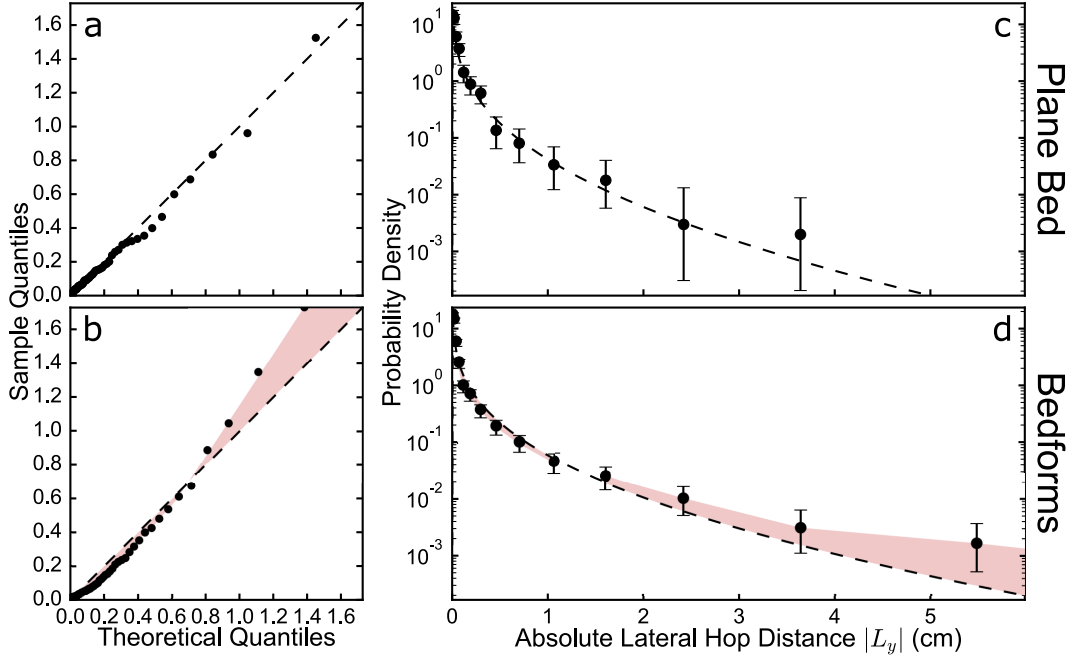


Figure 5. Quantile-quantile (a, b) and density plots (c, d) comparing measured distributions of absolute lateral hop distance with best-fit Weibull distributions with shape parameter $k = 1/2$ (dashed lines). Densities were computed using logarithmically-spaced bins. Error bars represent the 95% Bayesian credible interval for a binomial proportion obtained using Jeffrey’s prior (Brown et al., 2001). Red regions in panels (b) and (d) highlight systematic deviations from plane-bed theory.

551 average absolute lateral hop distance. This result primarily reflects an increase in the
 552 variability in transport direction as characterized by the coefficient of lateral transport
 553 (Table 1).

554 **4.4 Bedload Diffusion**

555 We have found that bedforms increase the variance of the ensemble probability dis-
 556 tributions of streamwise and absolute lateral hop distances. Here, we consider the sig-
 557 nificance of this observation in the context of macroscopic transport equations under the
 558 assumption that these moments are in fact finite and well-represented by our data. As
 559 noted previously, the Fokker-Planck approximation of the one dimensional entrainment
 560 flux consists of three terms: a local advective term that represents the mean hop distance,
 561 a nonlocal advective term that squared the squared mean, and a diffusive term that rep-
 562 represents the variance. These three terms are not guaranteed to map directly onto the typ-
 563 ical advective and diffusive terms contained in the activity form of the flux (Furbish et
 564 al., 2012, 2017), thus we refer to the sum of the first two terms as the advective-like flux
 565 and the third term as a diffusive-like flux.

566 Nonlocal advective-like and diffusive-like transport terms are zero under steady, uni-
 567 form transport conditions (Furbish et al., 2012). In order to compare the advective and
 568 diffusive behavior associated with a fixed distribution of particle hop distances, we con-
 569 sider a simple disequilibrium scenario in which the sediment flux varies due to a constant
 570 spatial gradient in the particle entrainment rate, $\partial E/\partial x = \beta$. In this case, the total

571 flux is steady, varying only as a function of x and is given by:

$$q_x(x) = E(x)\overline{L_x} - \frac{1}{2}\beta\overline{L_x}^{-2} - \frac{1}{2}\beta\sigma_{L_x}^2. \quad (9)$$

572 and the flux gradient is given by

$$\frac{\partial}{\partial x}q_x(x) = \beta\overline{L_x} \quad (10)$$

573 The diffusive flux is related to gradients in the advective flux by a diffusion length ℓ_{D_x}
 574 (Seizilles et al., 2014) as

$$q_{x,\text{diffusive}} = -\ell_{D_x}\frac{\partial}{\partial x}q_x(x). \quad (11)$$

575 For the simple disequilibrium conditions considered here, this diffusion length reduces
 576 to $\ell_{D_x} = \sigma_{L_x}^2/\overline{L_x}$.

577 If hop distances are assumed to follow a Weibull distribution with shape param-
 578 eter $k = 1/2$, the diffusion length is given by $\ell_{D_x} = 5\overline{L_x}$. The ratio of diffusion length
 579 to hop length $\ell_{D_x}/\overline{L_x}$ is like an inverse Peclet number in that it scales the relative propen-
 580 sity for diffusion-like and advection-like transport in the presence of gradients in parti-
 581 cle entrainment rate. We recognize that the entrainment rate and the probability dis-
 582 tributions of particle hop distance vary together in response to changes in boundary con-
 583 ditions; however, this mathematical abstraction is useful in that it enables a direct char-
 584 acterization of the effects of bedform development on particle diffusion.

585 For the plane bed experiment reported here, we find that measured distributions
 586 of particle hop distance lead to $\ell_{D_x} = 4.2\overline{L_x}$. Thus, the Weibull distribution proposed
 587 by previous authors appropriately predicts the measured relationship between stream-
 588 wise diffusion and streamwise advection for naturally sorted sediments transported over
 589 planar topography. In contrast, we find for the bedform condition that $\ell_{D_x} = 10.6\overline{L_x}$,
 590 deviating significantly from theory.

591 Following similar arguments presented above but assuming a constant lateral gra-
 592 dient in particle entrainment rate $\partial E/\partial y$, it is straightforward to show that the lateral
 593 diffusive flux is related to the lateral gradient in the streamwise advective flux by a dif-
 594 fusion length $\ell_{D_y} = \sigma_{L_y}^2/\overline{L_x}$. Though, we lack a clear basis for predicting the lateral
 595 diffusion length as we have done for the streamwise diffusion length above, we assume
 596 as a starting point that the lateral Peclet number is fixed over plane-bed topography (as
 597 theory predicts for the streamwise Peclet number). For measured particle hop distances
 598 over plane-bed topography, we find that $\ell_{D_y} = 1.07\overline{L_x}$. In contrast, particle motions
 599 in the bedform experiment have a lateral diffusion length of $\ell_{D_y} = 6.17\overline{L_x}$.

600 An important assumption in this analysis is that the distribution of particle hop
 601 distance is independent of the entrainment rate. Correlations between these variables
 602 cannot be evaluated using data reported here and may serve to enhance or diminish macro-
 603 scopic diffusion. Nevertheless, bedform development appears to increase the propensity
 604 for streamwise and lateral diffusive transport quantified by an inverse Peclet number that
 605 is equal to the squared coefficient of variation (for streamwise diffusion) or the squared
 606 coefficient of lateral transport (for lateral diffusion). This difference cannot be explained
 607 by an increase in shear stress alone which would likely cause an increase in the mean stream-
 608 wise hop distance (Lajeunesse et al., 2010). Instead, bedform development results in a
 609 decrease of the mean streamwise hop distance with a concurrent increase of the variance
 610 of streamwise and lateral hop distances in our experiments. The notion that this differ-
 611 ence is primarily caused by the development of bedform topography is entirely consis-
 612 tent with previously observed differences in particle behavior described by Wilson and
 613 Hay (2016), Leary and Schmeeckle (2017), Tsubaki et al. (2018), and Terwisscha van Scheltinga
 614 et al. (2019).

615 4.5 Experimental Censorship

616 We have interpreted these data as representative of the ensemble distribution of
 617 particle hop distances and travel times characteristic of macroscopic flow conditions. In
 618 principle, this requires an unbiased sample of particle motions representing all possible
 619 microconfigurations of flow, topography, and sediment transport. However, practical con-
 620 siderations limited the spatiotemporal extent over which it was possible to measure par-
 621 ticle motions. This has two effects which could potentially influence our results.

622 The first effect is related to the fact that particles with longer hop distances and
 623 travel times are more likely to begin or end their motions outside of the measurement
 624 window. This effect causes a systematic reduction in the sample mean and variance re-
 625 lative to the true mean and variance because hops are censored at a rate that is propor-
 626 tional to their duration and length. In order to evaluate the importance of this effect,
 627 we performed the correction proposed by Ballio et al. (2019). This correction resulted
 628 in almost no change in estimates of the mean or variance in either of our experiments.
 629 Although this correction cannot account for all forms of censorship (for example, trun-
 630 cation of the distribution), we are confident that our results are not substantially influ-
 631 enced by this effect.

632 The second effect concerns the fact that our sampling window is not large enough
 633 to capture a representative sample of particle motions originating from all possible mi-
 634 croconfigurations of flow and topography characteristic of the macroscopic transport con-
 635 ditions. The importance of this effect cannot be evaluated directly from available data.
 636 Nevertheless, we argue that our data are sufficient to provide unequivocal support for
 637 the primary claims made in this paper. Observed differences in particle behavior are con-
 638 sistent with previous studies of particle motion over bedforms (e.g., Wilson & Hay, 2016;
 639 Leary & Schmeeckle, 2017; Tsubaki et al., 2018) and qualitative differences illustrated
 640 in figure 1. Additionally, the mean lateral hop distance in the bedform experiment is ap-
 641 proximately zero (-0.028 cm) despite clear spatial correlations in lateral hop distance within
 642 the measurement window (Figure 1). Assuming the true mean lateral hop distance is zero,
 643 we tentatively interpret this as an indicator that the spatiotemporal extent of our mea-
 644 surement window is sufficiently large such that the measured statistics have begun to
 645 converge on the true ensemble statistics. By way of analogy, consider the problem of es-
 646 timating the mean and variance of bed elevation in a stable bedform field. Measurements
 647 from a single bedform will provide reasonable first-order estimates of these quantities de-
 648 spite the fact that there is variability between bedforms (Robert & Richards, 1988; Nikora
 649 et al., 1997).

650 We argue that the primary findings of this paper concerning the forms of the dis-
 651 tributions of particle hop distance and travel time over bedforms are robust to possible
 652 censorship effects. Increases in streamwise and lateral diffusivity are consistent with ob-
 653 servations of particle motion reported by previous authors cannot be explained by cen-
 654 sorship or sampling biases.

655 4.6 Limitations and Future Work

656 Our theoretical and experimental approach has several important limitations that
 657 must be addressed in order to extend the utility of our results to a wide range of macro-
 658 scopic morphodynamic modeling problems. Here, we outline these limitations and pro-
 659 vides suggestions for future studies focused on particle motions over bedforms.

660 The first limitation discussed in Section 3.3 is that measured distributions of par-
 661 ticle hop distance and travel time depend on the criterion used for differentiating between
 662 mobile and immobile particles. Bed elevation is also defined with respect to the positions
 663 of particles in the immobile phase such that different criteria potentially lead to differ-
 664 ent descriptions of topography. We report results obtained using a mobility criterion that

665 is consistent with previous work but ultimately subjective. Different criteria are valid
 666 as long as they obey mass conservation (i.e., mobile and immobile states encompass all
 667 particles and are mutually exclusive), and therefore provide alternative but compatible
 668 descriptions of sediment transport and morphodynamics. Recognizing this, the next step
 669 is to investigate how different choices of mobility criteria influence measured statistics
 670 of topography and particle motion. The morphodynamic interpretation of varying thresh-
 671 olds is similar to the scale-dependent active layer concept (Church & Haschenburger, 2017)
 672 and could potentially lead to valuable insights regarding interactions between fluctua-
 673 tions in bed elevation at the grain, bedform, bar, and channel scale (e.g., Nikora et al.,
 674 1997).

675 Another important issue is that the theoretical framework presented here is only
 676 valid for quasi-steady, uniform transport. In principle, this condition is satisfied if we con-
 677 sider macroscopic transport averaged over bedform-scale fluctuations (i.e., averaged over
 678 the bedform field timescale as envisioned by Furbish et al., 2012); however, an impor-
 679 tant caveat is that equations (4) and (5) assume that the entrainment rate and hop dis-
 680 tance are independent. This assumption is valid for planar topography because the en-
 681 trainment rate is effectively uniform, but bedforms potentially introduce correlations be-
 682 tween the entrainment rate and hop distance that can influence the macroscopic trans-
 683 port rate.

684 To clarify this point, consider that the entrainment rate may fluctuate under macro-
 685 scopically steady, uniform boundary conditions when bedforms are present. In this case,
 686 the instantaneous entrainment rate may be viewed as a probabilistic quantity and the
 687 ensemble average flux (over all possible topographic configurations) is given by $q_x = \overline{EL_x}$.
 688 This becomes $q_x = E\overline{L_x}$ if E is constant, or $q_x = \overline{E}\overline{L_x}$ if E and L_x are independent.
 689 If they are not independent, the flux may be expressed in terms of a mean and deviat-
 690 oric component as

$$q_x = \overline{E}\overline{L_x} + \overline{E'L'_x} \quad (12)$$

691 where $E' = E - \overline{E}$ and $L'_x = L_x - \overline{L_x}$. The second term in this expression is a covari-
 692 ance and can be rewritten as $\overline{E'L'_x} = \rho_{EL_x}\sigma_E\sigma_{L_x}$, where ρ_{EL_x} is the correlation co-
 693 efficient for the entrainment rate and hop distance, σ_E is the standard deviation of the
 694 entrainment rate, and σ_{L_x} is the standard deviation of the hop distance. The diffusive
 695 contribution to the flux under disequilibrium conditions may similarly be expanded in
 696 terms of mean and deviatoric components. This clarifies how correlations can influence
 697 the macroscopic transport rate and leads to several unanswered questions. First, are the
 698 entrainment rate and hop distance correlated over equilibrium mobile bedforms? Sec-
 699 ond, how does the correlation coefficient change under different conditions? Third, how
 700 do entrainment rate and hop distance vary within a statistically homogeneous bedform
 701 field as a function of local topography?

702 Because our experimental approach was aimed at quantifying the probability distri-
 703 bution of particle hop distance and travel time averaged over all possible topographic
 704 configurations, our results are limited in their capacity to elucidate the interaction be-
 705 tween particle motion and bedform evolution at the granular scale. Nevertheless, our re-
 706 sults clearly indicate that particle motions vary systematically in relation to topogra-
 707 phy. Future studies investigating this relationship may clarify (a) how morphodynamic
 708 feedbacks lead to a stable condition where the motion of individual particles perpetu-
 709 ates an statistically steady, uniform topographic configuration, and (b) how bedforms
 710 influence the advective and diffusive components of the flux under different flow condi-
 711 tions.

712 5 Conclusions

713 This paper presents results of an experimental study comparing the probability distri-
 714 butions that describe the spatiotemporal scales of particle motion linking particle en-

715 trainment and detrainment events. Measured distributions of particle travel time, T_p ,
 716 streamwise hop distance, L_x , and lateral hop distance, L_y , are compared with previously
 717 proposed theoretical distributions describing particle motions over plane-bed topogra-
 718 phy. We confirm that particle motions over plane-bed topography in natural sediments
 719 conform to existing theory. Travel times follow an exponential distribution while stream-
 720 wise and absolute lateral hop distances follow a Weibull distribution with shape param-
 721 eter $k = 1/2$.

722 In contrast, we find that particle hop distances over bedforms possess an increased
 723 standard deviation in both the streamwise and lateral directions relative to the mean stream-
 724 wise hop distance. We argue that this effect is consistent with observations of particle
 725 motion over bedforms reported by previous authors; quantities like particle activity and
 726 velocity vary systematically in relation to topographic position. Topographically-induced
 727 deviations from mean-particle behavior coupled with local flow velocity result in an ad-
 728 ditional source of variability that is superimposed on turbulent flow and particle colli-
 729 sion effects. At the macroscopic scale, this means that the relative magnitudes of advec-
 730 tive and diffusive-like transport implied by plane-bed distributions cannot be assumed
 731 when bedforms are present. Instead, bedforms increase the propensity for streamwise
 732 and lateral diffusion-like transport.

733 Acknowledgments

734 We thank the donors of the American Chemical Society Petroleum Research Fund 54492-
 735 DNI8, the National Science Foundation (NSF) grant EAR-1632938, and the University
 736 of Wyoming School for Energy Resources for partially supporting this research. We also
 737 thank Christophe Ancey, Francesco Ballio, David Furbish, and three anonymous review-
 738 ers for feedback that significantly improved this paper. Data and code are available through
 739 Figshare (Ashley et al., 2019).

740 References

- 741 Abbott, J. E., & Francis, J. R. D. (1977). Saltation and suspension trajectories of
 742 solid grains in a water stream. *Philosophical Transactions of the Royal Society*
 743 *of London. Series A, Mathematical and Physical Sciences*, *284*(1321), 225–254.
 744 doi: 10.1098/rsta.1977.0009
- 745 Abramian, A., Devauchelle, O., Seizilles, G., & Lajeunesse, E. (2019). Boltzmann
 746 distribution of sediment transport. *Physical Review Letters*, *123*(1). doi: 10
 747 .1103/PhysRevLett.123.014501
- 748 Ancey, C. (2010). Stochastic modeling in sediment dynamics: Exner equation for
 749 planar bed incipient bed load transport conditions. *Journal of Geophysical Re-*
 750 *search: Earth Surface*, *115*(F2), 1–21. doi: 10.1029/2009JF001260
- 751 Ancey, C., Bohorquez, P., & Heyman, J. (2015). Stochastic interpretation of the ad-
 752 vection diffusion equation and its relevance to bed load transport. *J. Geophys.*
 753 *Res:Earth Surf.*, *120*(12), 2529–2551.
- 754 Ancey, C., & Heyman, J. (2014). A microstructural approach to bed load transport:
 755 mean behaviour and fluctuations of particle transport rates. *Journal of Fluid*
 756 *Mechanics*, *744*, 129–168. doi: 10.1017/jfm.2014.74
- 757 Ashley, T. C., Mahon, R., Naqshband, S., Leary, K., & McElroy, B. (2019). *Parti-*
 758 *cle motions over plane-bed and bedform topography*. Figshare Dataset. doi: 10
 759 .6084/m9.figshare.11413038.v2
- 760 Bagherimiyab, F., & Lemmin, U. (2013). Shear velocity estimates in rough-bed
 761 open-channel flow. *Earth Surface Processes and Landforms*, *38*(14), 1714–1724.
 762 doi: 10.1002/esp.3421
- 763 Ballio, F., Pokrajac, D., Radice, A., & Hosseini Sadabadi, S. A. (2018). Lagrangian
 764 and Eulerian description of bed load transport. *Journal of Geophysical Re-*
 765 *search: Earth Surface*, *123*(2), 384–408. doi: 10.1002/2016JF004087

- 766 Ballio, F., Radice, A., Fathel, S. L., & Furbish, D. J. (2019). Experimental cen-
 767 sorship of bed load particle motions and bias correction of the associated fre-
 768 quency distributions. *Journal of Geophysical Research: Earth Surface*, *124*(1),
 769 116–136. doi: 10.1029/2018JF004710
- 770 Best, J. L. (1992). On the entrainment of sediment and initiation of bed defects: in-
 771 sights from recent developments within turbulent boundary layer research. *Sed-*
 772 *imentology*, *39*(5), 797–811. doi: 10.1111/j.1365-3091.1992.tb02154.x
- 773 Best, J. L. (2005). The fluid dynamics of river dunes: A review and some future
 774 research directions. *Journal of Geophysical Research: Earth Surface*, *110*(F4).
 775 doi: 10.1029/2004JF000218
- 776 Best, J. L. (2009). Kinematics, topology and significance of dune-related macro-
 777 turbulence: some observations from the laboratory and field. In M. D. Blum,
 778 S. B. Marriott, & S. F. Leclair (Eds.), *Fluvial sedimentology vii* (pp. 41–60).
 779 Oxford, UK: Blackwell. doi: 10.1002/9781444304350.ch3
- 780 Bradski, G. (2000). The OpenCV library. *Dr. Dobb’s Journal of Software Tools*, *25*.
- 781 Brown, L. D., Cai, T. T., & DasGupta, A. (2001, may). Interval Estima-
 782 tion for a Binomial Proportion. *Statistical Science*, *16*(2), 101–133. Re-
 783 trieved from <http://projecteuclid.org/euclid.ss/1009213286> doi:
 784 10.1214/ss/1009213286
- 785 Campagnol, J., Radice, A., Ballio, F., & Nikora, V. (2015). Particle motion and
 786 diffusion at weak bed load: accounting for unsteadiness effects of entrainment
 787 and disentrainment. *Journal of Hydraulic Research*, *53*(5), 633–648. doi:
 788 10.1080/00221686.2015.1085920
- 789 Charru, F., Andreotti, B., & Claudin, P. (2013). Sand ripples and dunes. *Annual*
 790 *Review of Fluid Mechanics*, *45*(1), 469–493. doi: 10.1146/annurev-fluid-011212
 791 -140806
- 792 Church, M., & Haschenburger, J. K. (2017, jan). What is the “active layer”? *Wa-*
 793 *ter Resources Research*, *53*(1), 5–10. Retrieved from [http://doi.wiley.com/](http://doi.wiley.com/10.1002/2016WR019675)
 794 [10.1002/2016WR019675](http://doi.wiley.com/10.1002/2016WR019675) doi: 10.1002/2016WR019675
- 795 Coleman, S. E., & Nikora, V. I. (2011). Fluvial dunes: Initiation, characterization,
 796 flow structure. *Earth Surface Processes and Landforms*, *36*(1), 39–57. doi: 10
 797 .1002/esp.2096
- 798 Coleman, S. E., Nikora, V. I., McLean, S. R., Clunie, T. M., Schlicke, T., & Melville,
 799 B. W. (2006). Equilibrium hydrodynamics concept for developing dunes.
 800 *Physics of Fluids*, *18*(10). doi: 10.1063/1.2358332
- 801 Costello, W. R. (1974). *Development of bed configurations in coarse sands* (Ph.D.
 802 Dissertation). Massachusetts Institute of Technology.
- 803 Fathel, S., Furbish, D., & Schmeeckle, M. (2016). Parsing anomalous versus normal
 804 diffusive behavior of bedload sediment particles. *Earth Surface Processes and*
 805 *Landforms*, *41*(12), 1797–1803. doi: 10.1002/esp.3994
- 806 Fathel, S., Furbish, D. J., & Schmeeckle, M. W. (2015). Experimental evidence
 807 of statistical ensemble behavior in bed load sediment transport. *Jour-*
 808 *nal of Geophysical Research: Earth Surface*, *120*(11), 2298–2317. doi:
 809 10.1002/2015JF003552
- 810 Fryberger, S. G., & Dean, G. (1979). Dune forms and wind regime. *U.S. Geological*
 811 *Survey Professional Paper 1052*, 137–170.
- 812 Furbish, D. J., Fathel, S. L., & Schmeeckle, M. W. (2016). Particle motions and
 813 bedload theory: The entrainment forms of the flux and the Exner equation. In
 814 *Gravel-bed rivers: Process and disasters* (chap. 4). Chichester: John Wiley and
 815 Sons.
- 816 Furbish, D. J., Fathel, S. L., Schmeeckle, M. W., Jerolmack, D. J., & Schumer,
 817 R. (2017). The elements and richness of particle diffusion during sediment
 818 transport at small timescales. *Earth Surface Processes and Landforms*, *42*(1),
 819 214–237. doi: 10.1002/esp.4084
- 820 Furbish, D. J., Haff, P. K., Roseberry, J. C., & Schmeeckle, M. W. (2012). A prob-

- 821 abilistic description of the bed load sediment flux: 1. Theory. *Journal of Geo-*
822 *physical Research: Earth Surface*, 117(F3). doi: 10.1029/2012JF002352
- 823 Furbish, D. J., & Schmeeckle, M. W. (2013). A probabilistic derivation of the
824 exponential-like distribution of bed load particle velocities. *Water Resources*
825 *Research*, 49(3), 1537–1551. doi: 10.1002/wrcr.20074
- 826 Furbish, D. J., Schmeeckle, M. W., Schumer, R., & Fathel, S. L. (2016). Prob-
827 ability distributions of bed load particle velocities, accelerations, hop dis-
828 tances, and travel times informed by Jaynes’s principle of maximum entropy.
829 *Journal of Geophysical Research: Earth Surface*, 121(7), 1373–1390. doi:
830 10.1002/2016JF003833
- 831 Ganti, V., Meerschaert, M. M., Foufoula-Georgiou, E., Viparelli, E., & Parker,
832 G. (2010). Normal and anomalous diffusion of gravel tracer particles in
833 rivers. *Journal of Geophysical Research: Earth Surface*, 115(F2), 1–12. doi:
834 10.1029/2008JF001222
- 835 García, M. H. (2008). Sediment transport and morphodynamics. In *Sedimen-*
836 *tation engineering* (pp. 21–163). Reston, VA: American Society of Civil Engi-
837 neers. doi: 10.1061/9780784408148.ch02
- 838 Gibbs, J. W. (1902). *Elementary principles in statistical mechanics*. New Haven:
839 Yale University Press.
- 840 Heyman, J., Bohorquez, P., & Ancey, C. (2016). Entrainment, motion, and depo-
841 sition of coarse particles transported by water over a sloping mobile bed. *Jour-*
842 *nal of Geophysical Research: Earth Surface*, 121(10), 1931–1952. doi: 10.1002/
843 2015JF003672
- 844 Hosseini-Sadabadi, S. A., Radice, A., & Ballio, F. (2019). On reasons of the scatter
845 of literature data for bed-load particle hops. *Water Resources Research*, 55(2),
846 1698–1706. doi: 10.1029/2018WR023350
- 847 Houssais, M., & Jerolmack, D. J. (2017). Toward a unifying constitutive relation for
848 sediment transport across environments. *Geomorphology*, 277, 251–264. doi:
849 10.1016/j.geomorph.2016.03.026
- 850 Houssais, M., Ortiz, C. P., Durian, D. J., & Jerolmack, D. J. (2015). Onset of sed-
851 iment transport is a continuous transition driven by fluid shear and granular
852 creep. *Nature Communications*, 6(1), 6527. doi: 10.1038/ncomms7527
- 853 Kwoil, E., Venditti, J. G., Bradley, R. W., & Winter, C. (2017). Observations
854 of coherent flow structures over subaqueous high- and low-angle dunes.
855 *Journal of Geophysical Research: Earth Surface*, 122(11), 2244–2268. doi:
856 10.1002/2017JF004356
- 857 Lajeunesse, E., Malverti, L., & Charru, F. (2010). Bed load transport in turbulent
858 flow at the grain scale: Experiments and modeling. *Journal of Geophysical Re-*
859 *search: Earth Surface*, 115(4). doi: 10.1029/2009JF001628
- 860 Le Bouteiller, C., & Venditti, J. G. (2015). Sediment transport and shear stress
861 partitioning in a vegetated flow. *Water Resources Research*, 51(4), 2901–2922.
862 doi: 10.1002/2014WR015825
- 863 Leary, K. C. P., & Schmeeckle, M. W. (2017). The importance of splat events to
864 the spatiotemporal structure of near-bed fluid velocity and bedload motion
865 over bedforms: Laboratory experiments downstream of a backward-facing step.
866 *Journal of Geophysical Research: Earth Surface*. doi: 10.1002/2016JF004072
- 867 Liu, M. X., Pelosi, A., & Guala, M. (2019). A statistical description of particle mo-
868 tion and rest regimes in open-channel flows under low bedload transport. *Jour-*
869 *nal of Geophysical Research: Earth Surface*, 124(11), 2666–2688. doi: 10.1029/
870 2019JF005140
- 871 Maddux, T. B., McLean, S. R., & Nelson, J. M. (2003). Turbulent flow over three-
872 dimensional dunes: 2. Fluid and bed stresses. *Journal of Geophysical Research:*
873 *Earth Surface*, 108(F1). doi: 10.1029/2003JF000018
- 874 Maddux, T. B., Nelson, J. M., & McLean, S. R. (2003). Turbulent flow over three-
875 dimensional dunes: 1. Free surface and flow response. *Journal of Geophysical*

- 876 *Research: Earth Surface*, 108(F1). doi: 10.1029/2003JF000017
- 877 McElroy, B. (2009). *Expressions and implications of sediment transport variability in*
878 *sandy rivers* (Ph.D. Dissertation). University of Texas, Austin.
- 879 McLean, S. R. (1990). The stability of ripples and dunes. *Earth-Science Reviews*,
880 29(1-4), 131–144. doi: 10.1016/0012-8252(0)90032-Q
- 881 Mclean, S. R., Nelson, J. M., & Wolfe, S. R. (1994). Turbulence structure over two-
882 dimensional bed forms: Implications for sediment transport. *Journal of Geo-*
883 *physical Research*, 99(C6), 12729–12747. doi: 10.1029/94JC00571
- 884 Muste, M., Baranya, S., Tsubaki, R., Kim, D., Ho, H., Tsai, H., & Law, D. (2016).
885 Acoustic mapping velocimetry. *Water Resources Research*, 52(5), 4132–4150.
886 doi: 10.1002/2015WR018354
- 887 Nakagawa, H., & Tsujimoto, T. (1976). On probabilistic characteristics of motion
888 of individual sediment particles on stream beds. In *Hydraulic problems solved*
889 *by stochastic methods: Second international iahr symposium on stochastic hy-*
890 *draulics* (pp. 293–320). Lund, Sweden: International Association of Hydraulic
891 Engineering and Research.
- 892 Naqshband, S., McElroy, B., & Mahon, R. C. (2017). Validating a universal
893 model of particle transport lengths with laboratory measurements of sus-
894 pended grain motions. *Water Resources Research*, 53(5), 4106–4123. doi:
895 10.1002/2016WR020024
- 896 Nikora, V. I., Habersack, H., Huber, T., & McEwan, I. (2002). On bed particle dif-
897 fusion in gravel bed flows under weak bed load transport. *Water Resources Re-*
898 *search*, 38(6). doi: 10.1029/2001WR000513
- 899 Nikora, V. I., Heald, J., Goring, D., & McEwan, I. (2001). Diffusion of saltating
900 particles in unidirectional water flow over a rough granular bed. *Journal of*
901 *Physics A: Mathematical and General*, 34(50). doi: 10.1088/0305-4470/34/50/
902 103
- 903 Nikora, V. I., Sukhodolov, A., & Rowinski, P. (1997). Statistical sand wave dynam-
904 ics in one-directional water flows. *Journal of Fluid Mechanics*, 351, 17–39. doi:
905 10.1017/s0022112097006708
- 906 Nordin, C. F. (1971). Statistical properties of dune profiles. *U.S. Geology Survey*
907 *Professional Paper 562-F*, 41.
- 908 Parker, G., Paola, C., & Leclair, S. (2000). Probabilistic Exner sediment continuity
909 equation for mixtures with no active layer. *Journal of Hydraulic Engineering*,
910 126(11), 818–826. doi: 10.1061/(ASCE)0733-9429(2000)126:11(818)
- 911 Parker, G., Seminara, G., & Solari, L. (2003). Bed load at low Shields stress on ar-
912 bitrarily sloping beds: Alternative entrainment formulation. *Water Resources*
913 *Research*, 39(7), 1–11. doi: 10.1029/2001WR001253
- 914 Pelosi, A., & Parker, G. (2014). Morphodynamics of river bed variation with vari-
915 able bedload step length. *Earth Surface Dynamics*, 2(1), 243–253. doi: 10
916 .5194/esurf-2-243-2014
- 917 Robert, A., & Richards, K. S. (1988). On the modelling of sand bedforms using the
918 semivariogram. *Earth Surface Processes and Landforms*, 13(5), 459–473. doi:
919 10.1002/esp.3290130510
- 920 Roseberry, J. C., Schmeckle, M. W., & Furbish, D. J. (2012). A probabilis-
921 tic description of the bed load sediment flux: 2. Particle activity and mo-
922 tions. *Journal of Geophysical Research: Earth Surface*, 117(F3). doi:
923 10.1029/2012JF002353
- 924 Rueden, C. T., Schindelin, J., Hiner, M. C., DeZonia, B. E., Walter, A. E., Arena,
925 E. T., & Eliceiri, K. W. (2017). ImageJ2: ImageJ for the next gener-
926 ation of scientific image data. *BMC Bioinformatics*, 18(1), 529. doi:
927 10.1186/s12859-017-1934-z
- 928 Schindelin, J., Arganda-Carreras, I., Frise, E., Kaynig, V., Longair, M., Pietzsch, T.,
929 ... Cardona, A. (2012). Fiji: an open-source platform for biological-image
930 analysis. *Nature Methods*, 9(7), 676–682. doi: 10.1038/nmeth.2019

- 931 Seizilles, G., Lajeunesse, E., Devauchelle, O., & Bak, M. (2014). Cross-stream diffu-
 932 sion in bedload transport. *Physics of Fluids*, *26*(1). doi: 10.1063/1.4861001
- 933 Simons, D. B., Richardson, E. V., & Nordin, C. F. (1965). Bedload equation for
 934 ripples and dunes. *Sediment Transport in Alluvial Channels, Geological Survey*
 935 *Professional Paper 462-H*, 1–9.
- 936 Southard, J. B., & Boguchwal, L. A. (1990). Bed configurations in steady uni-
 937 directional water flows. Part 2. Synthesis of flume data. *Journal of Sed-*
 938 *imentary Petrology*, *60*(5), 658–679. doi: 10.1306/212f9241-2b24-11d7
 939 -8648000102c1865d
- 940 Southard, J. B., & Dingler, J. R. (1971). Flume study of ripple propagation behind
 941 mounds on flat sand beds. *Sedimentology*, *16*, 251–263. doi: 10.1111/j.1365-
 942 -3091.1971.tb00230.x
- 943 Terwisscha van Scheltinga, R. C., Coco, G., & Friedrich, H. (2019). Sand parti-
 944 cle velocities over a subaqueous dune slope using high-frequency image cap-
 945 turing. *Earth Surface Processes and Landforms*, *44*(10), 1881–1894. doi:
 946 10.1002/esp.4617
- 947 Tinevez, J., Perry, N., Schindelin, J., Hoopes, G. M., Reynolds, G. D., Laplan-
 948 tine, E., . . . Eliceiri, K. W. (2017). TrackMate: An open and exten-
 949 sible platform for single-particle tracking. *Methods*, *115*, 80–90. doi:
 950 10.1016/j.ymeth.2016.09.016
- 951 Tsubaki, R., Baranya, S., Muste, M., & Toda, Y. (2018). Spatio-temporal patterns
 952 of sediment particle movement on 2D and 3D bedforms. *Experiments in Flu-*
 953 *ids*, *59*(6), 93. doi: 10.1007/s00348-018-2551-y
- 954 Tsujimoto, T. (1978). *Probabilistic model of the process of bed load transport and its*
 955 *application to mobile-bed problems* (Ph.D. Dissertation). Kyoto University, Ky-
 956 oto, Japan.
- 957 Tucker, G. E., & Bradley, D. N. (2010). Trouble with diffusion: Reassessing hillslope
 958 erosion laws with a particle-based model. *Journal of Geophysical Research*,
 959 *115*, 1–12. doi: 10.1029/2009jf001264
- 960 Van den Berg, J. H., & Van Gelder, A. (1993). A new bedform stability diagram,
 961 with emphasis on the transition of ripples to plane bed in flows over fine sand
 962 and silt. In *Alluvial sedimentation* (pp. 11–21). Oxford, UK: Blackwell Pub-
 963 lishing Ltd. doi: 10.1002/9781444303995.ch2
- 964 Van der Mark, C. F., & Blom, A. (2007). A new & widely applicable bedform track-
 965 ing tool. *Enschede, The Netherlands. University of Twente*, *31*.
- 966 Venditti, J. G., Church, M., & Bennett, S. J. (2005b). On the transition between 2D
 967 and 3D dunes. *Sedimentology*, *52*(6), 1343–1359. doi: 10.1111/j.1365-3091.2005
 968 .00748.x
- 969 Venditti, J. G., Church, M., & Bennett, S. J. (2006). On interfacial instability as a
 970 cause of transverse subcritical bed forms. *Water Resources Research*, *42*(7), 1–
 971 10. doi: 10.1029/2005WR004346
- 972 Venditti, J. G., Church, M. A., & Bennett, S. J. (2005a). Bed form initiation from
 973 a flat sand bed. *Journal of Geophysical Research: Earth Surface*, *110*(1), 1–19.
 974 doi: 10.1029/2004JF000149
- 975 Werner, B. T., & Kocurek, G. (1997). Bed-form dynamics: Does the tail wag
 976 the dog? *Geology*, *25*(9), 771–774. doi: 10.1130/0091-7613(1997)025<0771:
 977 BFDDTT>2.3.CO;2
- 978 Wilson, G. W., & Hay, A. E. (2016). Acoustic observations of near-bed sediment
 979 concentration and flux statistics above migrating sand dunes. *Geophysical Re-*
 980 *search Letters*, *43*(12), 6304–6312. doi: 10.1002/2016GL069579
- 981 Wong, M., & Parker, G. (2006). Reanalysis and correction of bed-load relation
 982 of Meyer-Peter and Müller using their own database. *Journal of Hydraulic*
 983 *Engineering*, *132*(11), 1159–1168. doi: 10.1061/(ASCE)0733-9429(2006)132:
 984 11(1159)
- 985 Wu, Z., Furbish, D., & Foufoula-Georgiou, E. (2020). Generalization of hop

986 distance-time scaling and particle velocity distributions via a two-regime for-
987 malism of bedload particle motions. *Water Resources Research*, 56(1). doi:
988 10.1029/2019WR025116